SPIE Reviews
an open access review journal
SPIEDigitalLibrary.org/reviews

Quantum-limited metrology with nonlinear detection schemes

Alfredo Luis

SPIE

Quantum-limited metrology with nonlinear detection schemes

Alfredo Luis
Complutense University of Madrid, Department of Optics, Faculty of Physical Sciences,
28040 Madrid, Spain
alluis@fis.ucm.es

Abstract. Quantum mechanics limit the resolution of detection schemes. Typical arrangements are based on linear processes, so that the corresponding quantum limits are usually understood as unsurpassable and ultimate. Recently it has been shown that nonlinear schemes allow signal detection and measurement with larger resolution than linear processes. In particular, this affects the quantum limits. We review the proposals introduced so far in this novel area of quantum metrology. [DOI: 10.1117/6.0000007]

Keywords: quantum metrology; uncertainty relations; nonclassical states; interferometry; quantum optics.

Paper SR100110 received Apr. 30, 2010; accepted for publication Aug. 1, 2010; published online Sep. 23, 2010.

1 Introduction

Quantum metrology investigates the ultimate limits that quantum physics places on the accuracy of the measurement of any magnitude, such as length, time, frequency, temperature, population, etc., referred to in general as the *signal*. Roughly speaking, the structure of detection schemes is quite universal. The signal modifies the state of a suitably prepared input probe state. This change is then detected by performing a measurement on the output probe state, whose outcome serves to estimate the value of the signal. By focusing on quantum limits, it is assumed that all sources of technical noise have been removed.

In standard metrology the signal induces linear transformations, so that previously known quantum limits heavily depend on the assumption of linearity. Thus, a new frontier arises if we consider that the signal can be imprinted in the probe via nonlinear processes. The key point is that nonlinear schemes allow us to reach larger resolutions than the linear ones. This leads to new quantum limits, new experiments, and eventually new devices. The improvement holds even when using probes in classical states, which is very relevant concerning robustness against practical imperfections.

Nonlinear transformations have played a distinguished role in quantum metrology, being extensively used for the preparation of nonclassical probe states (typically squeezed states), while signal transformation was always assumed to be linear. Nonlinear detection schemes change this perspective by showing that it is more advantageous to use nonlinear transformations to imprint the signal on the probe.

The objective of this review is to examine the work exploring this possibility [1–25]. Also, we hope to provide a quick start on the subject for newly interested readers. Technical details are deferred to appendices in Secs. 6, 7, and 8.

2 Quantum Metrology

Every quantum detection scheme contains five ingredients (see Fig. 1): the system, the input probe state, the transformation induced by the signal, the measurement performed on the output probe state, and the data analysis of the measurement outcomes.

1946-3251/2010/$25.00 © 2010 SPIE

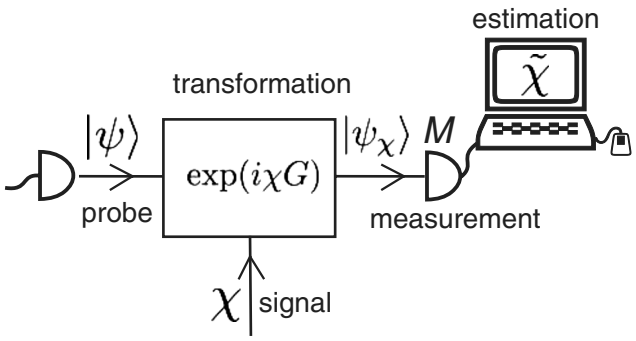

Fig. 1 Detection schemes.

2.1 *System*

The first step is to identify elementary physical systems sensitive enough to changes induced by the signal. Two main possibilities have been considered in the bibliography: quantum light and atoms, usually in Bose-Einstein condensates (for more details, see the proposals reviewed in Sec. 4.1). Fortunately, the quantum theory allows us to describe them in a unified fashion. When the system is made of identical particles (light and Bose-Einstein condensates), we use bosonic annihilation operators a_j representing the complex amplitude of the allowed modes (i.e., the degrees of freedom of the particles). Usually just two modes are considered, in which case the angular-momentum operators $\boldsymbol{J}$ are very useful (see Appendix A in Sec. 6). These are Stokes operators for light beams or collective spin operators for atoms. They allow us also to represent collections of distinguishable particles. For more details, see Appendix A in Sec. 6.

2.2 *Input Probe State*

The system is prepared in a probe state $|\psi\rangle$ (assumed pure for simplicity) that undergoes the transformation caused by the signal. The probe can be either in a classical or nonclassical state, usually entangled (see Appendix B in Sec. 7). The main advantage of nonclassical states is that they can provide better accuracy. The main advantage of classical states is that they are more robust against practical imperfections. Throughout this work probe realizations are assumed as statistically independent.

2.3 *Transformation*

Information about the signal χ is imprinted in the probe state by letting it experience a signal-dependent transformation $|\psi\rangle \rightarrow |\psi_\chi\rangle$. For simplicity we assume that the transformation is unitary

$$|\psi_\chi\rangle = \exp(i\chi G)\,|\psi\rangle, \tag{1}$$

where the generator G is Hermitian. A key point of this work is to distinguish between linear and nonlinear transformations.

2.3.1 *Linear transformations*

By linear transformations, we mean that the output complex amplitudes $\exp(-i\chi G)a_j \exp(i\chi G)$ are linear functions of the input ones a_j, maybe including their Hermitian conjugates $a_j^\dagger$. In such a case the generators G are at most quadratic polynomials of a_j, $a_k^\dagger$. Typical examples are phase shifts, generated by the number operator $\hat{n} = a^\dagger a$, and rotations of the angular-momentum operators $\boldsymbol{J}$, generated by a $\boldsymbol{J}$ component, say J_z. For two-level atoms this is $J_z \propto \Sigma_k \sigma_z^{(k)}$, where

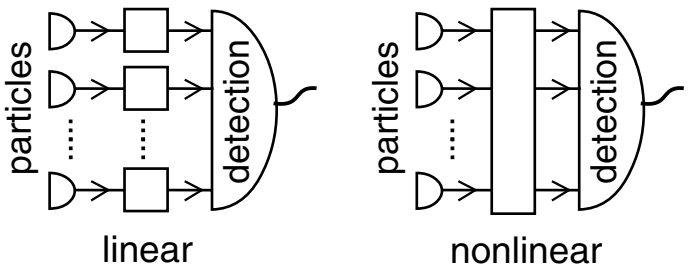

Fig. 2 Linear versus nonlinear schemes.

k indexes atoms and $\sigma^{(k)}$ are the Pauli matrices acting on the two-level space of each particle. Linear transformations correspond to free evolution, light propagation through optically linear media, beamsplitting, phase shifting, the most common interferometers, and atoms driven by external fields. Thus, most detection processes in interferometry and spectroscopy are linear.

2.3.2 *Nonlinear transformations*

By nonlinear transformations, we mean that the output complex amplitudes are not linear functions of the input ones. Their generators contain combinations of $a_j,\ a_k^\dagger$ with powers above the second. The most simple examples are $G = \hat{n}^2$ and $G = J_z^2$. For light, this corresponds to propagation through optically nonlinear media (such as the Kerr effect). In terms of single-atom operators, $J_z^2 \propto \Sigma_{k,\ell}\sigma_z^{(k)}\sigma_z^{(\ell)}$ includes two-body interactions (see Sec. 4.1).

Roughly speaking, in linear transformations each particle experiences the same transformation independent of the presence of other particles, irrespectively of whether the particles are prepared in independent or collective states (see Fig. 2). This can be exemplified by the famous saying that each photon interferes with itself [26]. In nonlinear schemes, particles interact among themselves during the imprinting of the signal, so that they experience a collective transformation.

2.4 *Measurement*

The signal information encoded in the output probe state $|\psi_\chi\rangle$ must be disclosed by a measurement M with statistics

$$P(m|\chi) = \left|\langle m|\psi_\chi\rangle\right|^2, \tag{2}$$

where $P(m|\chi)$ is the conditional probability of obtaining the outcome m when the true but unknown value of the signal is χ, and we have assumed for simplicity projection on pure states $|m\rangle$, usually the eigenstates of the measured observable $M|m\rangle = m|m\rangle$. In practical terms this is always a counting of atoms or photons per mode; this is $M = \hat{n}_j,\ J_z$. This is usually done after a linear coupling so that output populations depend via interference on the signal-induced phase shifts. The only exceptions seem to be the measurement of field quadratures $X \propto a + a^\dagger$ [4, 5], J_z^2 [to avoid the vanishing of $\langle J_z\rangle$ for strong SU(2) squeezed probes] [4,9], parity [8], and phase difference [9]. Nevertheless, more or less directly these are also always particle-counting measurements.

2.5 *Inference*

The last goal is to obtain the best hypothesis $\tilde{\chi}$ about χ along with its uncertainty $\Delta\tilde{\chi}$. Both should be derived from the statistics $P(m|\chi)$ of the measurement. In this work we are mainly interested in $\Delta\tilde{\chi}$, since this allows us to compare the performance of different schemes. The estimation of the uncertainty can be done in many different ways. The most popular are recalled

in Appendix C in Sec. 8. This subject is not trivial, since different data analysis can lead to different, or even contradictory, conclusions.

Nevertheless, for the purpose of this work it is enough to mention that most approaches lead essentially to a minimal signal uncertainty of the form

$$\Delta\tilde{\chi} = \frac{1}{2\sqrt{\nu}\Delta G}, \qquad (\Delta G)^2 = \langle\psi|G^2|\psi\rangle - \langle\psi|G|\psi\rangle^2, \tag{3}$$

and ν is the number of independent repetitions of the measurement. Leaving aside the statistical factor ν, this recalls a Heisenberg-kind of uncertainty relation $\Delta\tilde{\chi}\Delta G \geq 1/2$, although $\Delta\tilde{\chi}$ is not necessarily the variance of an operator.

3 Quantum Limits

The idea of precise detection is to have $\Delta\tilde{\chi}$ be as small as possible; this is ΔG as large as possible. If no further restrictions are placed, nothing would prevent acquiring ΔG as large as desired, so there would be no limit to accuracy [27]. Quantum limits can only emerge when we impose constraints. The most popular is to consider a fixed number of particles, although time limitations might also be considered [14,28] (see also Sec. 4.3). This is reasonable, since the number of available photons and atoms during the duration of the measurement seems to be always limited, for example, because of the maximum output power of lasers at hand. Nevertheless, this constraint is not trivial, since, for example, the quadrature coherent states have by definition an unbounded number of particles. Thus, there is the ambiguity of whether we refer to constraints in the total number or in the mean number. Because of this it can be advantageous to split the analysis for bounded and unbounded numbers of particles.

3.1 *Bounded Number of Particles*

Let us say that we have just N particles. This is tantamount to say that the Hilbert space of the problem is of finite dimension, and thus G is bounded. In such a case the maximum ΔG is reached by a 50% coherent superposition of the eigenstates of G, $|G_{\max,\min}\rangle$, with maximum and minimum eigenvalues $G_{\max,\min}$ [28]

$$\Delta G = \frac{1}{2}\left(G_{\max} - G_{\min}\right), \quad |\psi\rangle = \frac{1}{\sqrt{2}}\left(|G_{\max}\rangle + |G_{\min}\rangle\right). \tag{4}$$

Let us particularize this to linear and nonlinear schemes.

3.1.1 *Linear schemes*

To be more specific, let us consider $G = J_z$ as the generator so that (see Appendix A in Sec. 6 for more details)

$$G_{\max} = -G_{\min} = \frac{N}{2}, \quad \Delta G = \frac{N}{2}, \tag{5}$$

where the optimum probe state (in the angular-momentum basis $|j,\ m\rangle$) and the optimum resolution are

$$|\psi\rangle = \frac{1}{\sqrt{2}}\left(|j,\ j\rangle + |j,-j\rangle\right), \qquad \Delta\tilde{\chi} = \frac{1}{\sqrt{\nu}N}. \tag{6}$$

This can be compared with the maximum ΔG and minimum $\Delta\tilde{\chi}$ achievable when the probe is in a classical state. This is an equatorial SU(2) coherent state with polar angle $\theta = \pi/2$,

leading to

$$\Delta G = \frac{\sqrt{N}}{2}, \qquad \Delta\tilde{\chi} = \frac{1}{\sqrt{\nu N}}. \tag{7}$$

Let us draw some conclusions.

1. According to Eq. (6), the minimum uncertainty $\Delta\tilde{\chi}$ scales as the inverse of the number of particles N. This is usually referred to as the Heisenberg limit [28–40], considered the best that can be done with linear schemes. Nevertheless, other schemes where the probe state $|\psi\rangle$ may be different for different repetitions can achieve a better use of resources, leading to uncertainties $\Delta\tilde{\chi}$ scaling as $1/(\nu\, N)$ [40–43].
2. The optimum resolution requires the probe to be prepared in a maximally entangled state (i.e., it cannot be expressed as a product of states in the corresponding modes) $|\psi\rangle \propto |j, j\rangle + |j, -j\rangle$ in the angular-momentum basis, equivalent to $|\psi\rangle \propto |N\rangle_1|0\rangle_2 + |0\rangle_1|N\rangle_2$ in the particle-number basis. This is a coherent superposition of extreme distinguishable states, with all particles in one mode or the other (Schrödinger cat states or N00N states) [28,29,42–50].
3. As an alternative to the N00N states, the Heisenberg limit can also be approached by probes prepared in SU(2) squeezed states [9,51–59].
4. When using probes in coherent states (this is often regarded as equivalent to unentangled particles), the uncertainty in Eq. (7) scales as the inverse of the square root of the number of particles. This uncertainty is much larger than the Heisenberg limit in Eq. (6), referred to as the standard quantum limit [29,60].
5. Some approaches to quantum linear metrology propose to reach the Heisenberg limit with classical states [14,28,42,43,61,62] by using multiround or sequential protocols, where the same probe experiences the same signal-induced transformation several times. As stated in Ref. 14, the number of interactions is a discrete version of the evolution time τ. Increasing evolution time generally improves sensitivity, since $\chi \propto \tau$. As pointed out in Ref. 28, multiround protocols are an example of the frequent interplay between time and entanglement in quantum information. From a different perspective, this can be regarded as signal amplification with gain given by the number of rounds. Incidentally, nonlinear schemes might be regarded also as operating via signal amplification, as discussed in detail in Sec. 4.3.

   In any case, it seems that a proper comparison between different schemes (this is with different $|\psi\rangle$ and G) should be done on an equal-time basis, considering the same number of applications of the transformation. When this is done it arises that for linear schemes, resolution beyond coherent states requires nonclassical probes [21].

3.1.2 *Nonlinear schemes*

To be more specific, we consider $G = J_z^2$ so that, for $N \gg 1$,

$$G_{\max} = \frac{N^2}{4} \gg G_{\min}, \tag{8}$$

and

$$\Delta G = \frac{N^2}{8}, \quad \Delta\tilde{\chi} = \frac{4}{\sqrt{\nu}N^2}. \tag{9}$$

Thus, with the same number of particles N, the uncertainty in nonlinear schemes can be much smaller than in linear schemes, so we can say that nonlinear schemes provide resolution

beyond the Heisenberg limit. It might be argued that for different generators the Heisenberg limit should be different [24]. Leaving aside terminology, we stress that the key point is the different dependence on the number of particles N in Eqs. (6) and (9).

Also, for nonlinear schemes optimum resolution requires entangled probes, perhaps with the only exception of the scheme proposed in Ref. 12. The optimum uncertainty can be approached also using SU(2) squeezed states [9].

When considering probes prepared in SU(2) coherent states, the maximum variance for J_z^2 is obtained for $\theta = \pi/4$, leading to [10]

$$\Delta G = \frac{N^{3/2}}{4}, \qquad \Delta\tilde{\chi} = \frac{2}{\sqrt{\nu}N^{3/2}}. \tag{10}$$

This uncertainty is larger than Eq. (9), although this is still $\sqrt{N}$ times smaller than the Heisenberg limit in Eq. (6). We emphasize that this is perhaps the key point of nonlinear detection schemes: improvement of resolution by robust classical states.

3.2 *Unbounded Number of Particles*

When there is no restriction on the total number of particles, we have that G is usually unbounded, so there is no way to establish an upperbound on ΔG, even for a fixed mean number of particles [27,38–40]. As a very simple example let us consider the variance of the number operator $G = \hat{n}$ in the probe state (in the photon-number basis)

$$|\psi\rangle = \sqrt{1-p}|0\rangle + \sqrt{p}|n/p\rangle, \tag{11}$$

where $1 \geq p > 0$. It should be understood that n/p is an integer. The mean number of photons is $\langle\hat{n}\rangle = n$ for all p, while its uncertainty is

$$\Delta\hat{n} = n\sqrt{\frac{1-p}{p}}. \tag{12}$$

Therefore, when $p \to 0$, we have $\Delta\hat{n} \to \infty$. It seems that we would have arbitrarily high resolution $\Delta\tilde{\chi} \to 0$ with any fixed mean number of photons $\langle\hat{n}\rangle = n$, in contradiction with the usual idea of quantum limit. In a similar approach, Ref. 63 claims to beat the Heisenberg limit in a linear scheme with $G = J_x$ if the probe is prepared in the mixed state (in the photon-number basis)

$$\rho = (1-p)|0,0\rangle\langle 0,0| + p|n/p, n/p\rangle\langle n/p, n/p|, \tag{13}$$

where $|n_1, n_2\rangle = |n_1\rangle_1|n_2\rangle_2$ and n/p is an integer, leading to

$$(\Delta J_x)^2 = \frac{1}{2}\left(\frac{n^2}{p} + n\right), \qquad \langle\hat{N}\rangle = 2n, \tag{14}$$

so that again $\Delta J_x \to \infty$ when $p \to 0$ for a constant mean number of photons.

This seems paradoxical, since in both examples for $p \to 0$ the probe tends to be in the vacuum state, which is fully insensitive to phase changes. This recalls a similar difficulty when using reciprocal peak likelihood [27,64,65]. Perhaps the reason for this behavior is the nonlinearity of Fisher information and variance that overestimates the contribution of large photon numbers, even if their probabilities are small. This has prompted the investigation of other measures of fluctuations [66–79]. We do not discuss to what extent Eqs. (12) and (14) are meaningful results. In particular, this would affect equally linear and nonlinear schemes, so this is not crucial for the objectives of this work. Thus, *cum granum salis*, perhaps we should refer to Heisenberg *scaling*

rather than to the Heisenberg *limit* to emphasize the dependence with the number of particles, rather than claim the existence of an absolute lower bound.

Leaving aside these details, most analyses assume that the same limits of the bounded case hold simply by replacing the total number N by the mean number of particles $\langle \hat{N} \rangle$ or $\langle \hat{n} \rangle$. Concerning nonlinear schemes, the most simple example in the single-mode case is $G = \hat{n}^k$. Variance scaling as $\Delta G \propto \langle \hat{n} \rangle^k$ can be reached by quadrature squeezed states, while quadrature coherent states lead to $\Delta G \propto \langle \hat{n} \rangle^{k-1/2}$ [7,10,16].

Within this same framework, it has been shown that in nonlinear schemes, mixed classical states can lead to larger resolution than quadrature coherent states [21], which are pure states, contrary to what happens in linear schemes. This is revealed by the following probe state with density matrix

$$\rho = (1-p)|0\rangle\langle 0| + p|\alpha/\sqrt{p}\rangle\langle \alpha/\sqrt{p}|, \tag{15}$$

where $|\alpha/\sqrt{p}\rangle$ is a coherent state, $|0\rangle$ is the vacuum, and $1 \geq p > 0$, which includes the coherent state $|\alpha\rangle$ for $p = 1$. The mean number of photons is the same $\langle \hat{n} \rangle = |\alpha|^2$ for every p. For $G = \hat{n}^2$ and $|\alpha| \gg 1$, it holds that

$$\Delta G = 2\frac{\langle \hat{n} \rangle^{3/2}}{p}, \qquad \Delta \tilde{\chi} = \frac{p}{4\sqrt{\nu}\langle \hat{n} \rangle^{3/2}}, \tag{16}$$

so that $\Delta\tilde{\chi} \to 0$ as $p \to 0$, always with the same fixed mean number of particles. By contrast, in the linear scheme $G = \hat{n}$ for the same probe in Eq. (15) we get that $\Delta\tilde{\chi}$ does not depend on p.

This recalls the prior paradox around Eqs. (12) and (14). However, in this case there is a simple reasoning showing that this is a fully meaningful result. The ν times repetition of the measurement with the probe in Eq. (15) is equivalent to νp repetitions with probe $|\alpha/\sqrt{p}\rangle$. Since nonlinearity greatly benefits large photon numbers, the best strategy is to put as many photons as possible together, even at the price of getting fewer useful runs, say up to $\nu p \sim 1$. This behavior cannot be attributed to variance features, since it does not hold in the linear case.

4 Nonlinear Detection Schemes

Next we provide a more detailed account of the material published on quantum limits of nonlinear detection schemes, commenting on some specific items.

4.1 *Practical Implementations*

Essentially three basic schemes have been considered: atom-light interaction, light-light coupling via nonlinear optics, and atom-atom interactions, typically in Bose-Einstein condensates. Only the proposal in Ref. 14 dealing with nanomechanical resonators is somewhat out of this scope, although it can be clearly pictured as a nonlinear interferometer.

4.1.1 *Atom-light interaction*

Most proposals based on atom-light interactions are nonresonant, with a typical generator $G = \hat{n}J_z$, where J_z refers to a component of the collective atomic spin [1–3]. This is essentially the same transformations arising in Faraday rotation [80–82] and the basis of signal amplification further discussed in Sec. 4.3. In Ref. 3 there is a slight variation in the form $G = XJ_z$, where $X \propto a + a^\dagger$ is a field quadrature, that can be obtained from $G = \hat{n}J_z$ by a large displacement of the field complex amplitude a.

Reference 12 proposes a generalized resonant Jaynes-Cummings model, where a light mode of frequency $N\omega$ interacts with a molecule made of N two-level atoms of internal energies $\hbar\omega$,

via a coupling of the form

$$G \propto a \bigotimes_{k=1}^{N} \left[\sigma_x^{(k)} + i\sigma_y^{(k)}\right] + \text{HC}, \tag{17}$$

where $\sigma_{x,y}^{(k)}$ are the Pauli matrices for the k'th atom, and HC means Hermitian conjugated. This coupling produces the following evolution when the initial atomic state is $|j,\ m = j\rangle$ (i.e., all particles in the same mode),

$$e^{i\chi G}|j,\ j\rangle \rightarrow \cos\left(2^{N-1}\chi\right)|j,\ j\rangle - i\sin\left(2^{N-1}\chi\right)|j,\ -j\rangle. \tag{18}$$

As pointed out in Ref. 6, in this case the generator depends on N, so that when the number of atom changes, the interaction changes, which is somewhat peculiar. This might be the reason why this scheme reaches a resolution scaling exponentially $\Delta\tilde{\chi} = 1/2^N$ instead of the most typical polynomial form.

Within this same framework we can place the proposals of the magnetometer in Refs. 17 and 18, where a far-detuned laser beam passes twice through an atomic sample as it undergoes the Larmor precession, continuously observing the polarization of the light beam using techniques of quantum filtering. As stated by the authors, this double-pass scheme mimics a nonlinear magnetic interaction, although it is not trivial to explain the emergence of nonlinearity from effective linear couplings and formulate it resembling more typical nonlinear or multibody interactions.

Finally, the approach in Refs. 22 and 25 considers a near-resonant atom-light interaction leading to coupling terms of the form $G \propto S_\ell J_k + S_m^2 J_n$, where S_ℓ are field Stokes operators and J_k are components of the collective atomic spin, with the possibility of tuning the linear and nonlinear parts. Within this scheme, Ref. 25 presents an experimental demonstration of the sensitivity scaling in Eq. (10) obtained by letting pulses of polarized light interact with an ensemble of 10^6 cold ^{87}Rb atoms in a dipole trap, and probing one component of the collective angular momentum via measurements of the polarization changes in the light.

4.1.2 *Nonlinear optics*

Typical effective generators for light propagation in nonresonant nonlinear media are given by powers and products of photon-number operators of the form $G = \hat{n}^k$ in a single-mode approach [4,5,7,8,16,24], $G = J_z^2$ in a two-mode scheme [4], $G = \otimes_j^k \hat{n}_j$ in a multimode configuration [7], or even $G = \Sigma_j \hat{n}_j^k$ [23].

4.1.3 *Bose-Einstein condensates*

Most of the proposals based on atomic systems focus on two-mode Bose-Einstein condensates [6,9–11,13,15,19], where each mode corresponds to a different internal atomic state, typically two hyperfine levels. The most common generator is of the form $G = J_z^2$, arising from two-body collisions. Nevertheless, under some specific circumstances nonlinear terms of the form J_z^2 can be negligible, and the relevant leading term can be of the form $G = \hat{N} J_z$ [13,15,19], which is extremely interesting concerning the role of entanglement and amplification, as shown later. The signal χ is the strength of the two-body interaction being proportional to the scattering lengths. They can be tuned by varying an external magnetic field, and depend on the electron-to-proton mass ratio [9]. In Refs. 13,15, and 19, there are complete analyses of potential problems and challenges of such implementation, including the dependence of the nonlinear coupling with the number of atoms. In Refs. 6 and 10, there are very general analyses in terms of generators involving symmetric k-body terms. In Ref. 9, the implementation via fermionic atoms in an optical lattice loaded with one atom per site is discussed, with the advantage that losses are suppressed.

4.2 *Role of Entanglement*

Entanglement enters at two stages: entanglement carried by the probe and entanglement caused by the nonlinear transformation during detection.

4.2.1 *Entangled probes*

As we have shown in Sec. 3.1, optimum probes are usually entangled [28,29,83,84]. The only exception is in the proposal in Ref. 12, where the optimum resolution is seemingly reached by a separable probe.

For linear schemes, improved resolution beyond the one provided by coherent states requires first and foremost nonclassicality of the probe [21,85] (the situation is different for nonlinear schemes, as shown in Sec. 3.2 [21]). In turn, for distinguishable two-level particles, nonclassicality is equivalent to entanglement, because all states in 2-D spaces are classical [59]. For identical particles such as photons or Bose-Einstein condensates, the role of entanglement is much more obscure. On the one hand, entanglement plays no role in single-mode schemes. On the other hand, for two-mode schemes there are mode-factorized nonclassical states $|\psi_1\rangle|\psi_2\rangle$, where $|\psi_j\rangle$ is in the mode with complex amplitude a_j (such as the product of quadrature squeezed states) that reach Heisenberg scaling [86]. Thus, it seems that the key point for improved resolution is nonclassicality rather than entanglement.

From a more practical perspective, most analyses focus on the resolution achievable with classical or separable probes. Actually, there are few works considering in some detail nonclassical or entangled probes. In Ref. 9, the probe is prepared in an SU(2) squeezed state reaching maximum resolution for $G = J_z^2$, while in Ref. 16, quadrature squeezed probes are considered in a single-mode configuration with $G = \hat{n}^k$, showing that they can reach maximum resolution with the same amount of squeezing for all k.

4.2.2 *Signal-induced entanglement*

It has been debated whether the improved resolution provided by nonlinear schemes is due to entanglement caused by the signal-induced nonlinear transformation during the detection process, as more or less directly suggested in Refs. 6,9, and 12. In fact, the same nonlinear generators considered here for the signal transformation were proposed previously to produce the nonclassical probes reaching optimum resolution in linear schemes.

However, there are some conclusive arguments showing that entanglement plays no role, and even might be counterproductive [7,10,11,13,15,23]. A very first proof is provided by the single-mode schemes in quantum optics [1–5,8,16], since for single-mode photons there is no room for entanglement. Moreover, in Ref. 7 there is a simple comparison between single-mode and multimode configurations showing that, *ceteris paribus*, single-mode transformations provide better performance than multimode entangling ones. A similar conclusion has been reached in Ref. 23, showing that for nonlinear generators the best strategy is to concentrate all resources in a single mode instead of splitting them over many modes.

Further conclusive proofs are provided in Refs. 10 and 13. In Ref. 10 there is a very illustrative model showing that signal-generated entanglement becomes negligible (see the linearization in Sec. 4.3). An even more convincing argument is presented in Ref. 13, where a generator $G = \hat{N} J_z$ is suitably engineered, where $\hat{N}$ is the total number operator, so that the signal-induced transformation does not produce entanglement at all. Moreover, it is argued in Refs. 11,13, and 15 that entanglement may lead to phase dispersion that, far from being an aid, prevents reaching optimum resolution.

Next we discuss that built-in signal amplification, rather than entanglement, serves to account for the improved performance of nonlinear schemes.

4.3 *Phase Amplification*

Here we present an intuitive picture of the enhancement of resolution caused by nonlinear processes. Let us consider the simplest single-mode situation, comparing the linear $G = \hat{n}$ and nonlinear schemes $G = \hat{n}^2$, with a probe in a coherent state $|\alpha\rangle$ in both cases. In the linear arrangement, the mean value of the complex amplitude in the transformed state is

$$\langle\psi_\chi|a|\psi_\chi\rangle = \alpha e^{i\chi}, \quad |\psi_\chi\rangle = \exp(i\chi G)|\alpha\rangle, \tag{19}$$

where $|\psi_\chi\rangle = \exp(i\chi\hat{n})|\alpha\rangle = |\alpha e^{i\chi}\rangle$ is a coherent state with complex amplitude $\alpha\exp(i\chi)$. On the other hand, in the nonlinear case with $G = \hat{n}^2$, we have

$$\langle\psi_\chi|a|\psi_\chi\rangle = \alpha e^{i\chi}\langle\alpha|\alpha e^{i2\chi}\rangle = \alpha e^{i\chi}e^{-2|\alpha|^2\sin^2\chi}e^{i|\alpha|^2\sin(2\chi)}, \tag{20}$$

where we have used $af(\hat{n}) = f(\hat{n}+1)a$. This can be simplified if $\chi \ll 1$ and $|\alpha|\chi \ll 1$

$$\langle\psi_\chi|a|\psi_\chi\rangle \simeq \alpha e^{i2\langle\hat{n}\rangle\chi}, \tag{21}$$

with $\langle\hat{n}\rangle = |\alpha|^2$. Comparing Eqs. (19) and (21), we see that in the nonlinear case there is an effective and noiseless amplification of the signal $\chi \to 2\langle\hat{n}\rangle\chi$ [1,2,13], which is referred to as increased or enhanced rotation in Refs. 10 and 15. The signal amplification is also very clear in Ref. 12 [see Eq. (18)]. Moreover, in Refs. 17 and 18, it is explicitly stated that the improvement arises from amplification of the Larmor precession.

A different approximation leading to an equivalent conclusion for our purposes considers, prior to performing any transformation, the linearization of $\hat{n}^2$ around its mean value (roughly speaking valid provided that $\Delta\hat{n} \ll \langle\hat{n}\rangle$),

$$\hat{n}^2 \simeq \langle\hat{n}\rangle^2 + 2\langle\hat{n}\rangle(\hat{n} - \langle\hat{n}\rangle) \to 2\langle\hat{n}\rangle\hat{n}, \tag{22}$$

where the constant terms $\langle\hat{n}\rangle^2$ can be ignored, since they lead to global phases that play no essential role. This is the uniform-fringe approximation $J_z^2 \to 2\langle J_z\rangle J_z$ considered in Refs. 10 and 15. Within this limit both phase dispersion and signal-induced entanglement disappear, and an initial coherent probe state remains always coherent $|\psi_\chi\rangle \simeq |\alpha\exp(i2\langle\hat{n}\rangle\chi)\rangle$.

4.3.1 *Phase ambiguity*

Phase-shift amplification unavoidably implies signal ambiguity, since in the previous example in Eq. (21) we have that χ and $\chi + \pi/\langle\hat{n}\rangle$ produce the same effects. This parallels the free spectral range in spectroscopic measurements using Fabry-Perot interferometers or diffraction gratings. It can be avoided by suitably distributing the measurement into several steps of different precision [10,40–43,61,62]. Otherwise, the signal must be known with a prior uncertainty of the order of $1/\langle\hat{n}\rangle$. The posterior resolution after ν repetitions of the measurement with the probe in a coherent state is of the order of $1/(\sqrt{\nu}\langle\hat{n}\rangle^{3/2})$, so even in such a case there is an improvement of resolution by a factor $\sqrt{\nu\langle\hat{n}\rangle}$ from the prior to posterior situations.

4.4 *Robustness Against Practical Imperfections*

A relevant feature of nonlinear detection is the possibility of reducing uncertainty with classical probe states. This is an interesting property, because nonclassical states tend to be fragile against practical imperfections [87–90]. Thus, unlike other applications of quantum theory, quantum metrology might not face formidable problems fighting decoherence [12]. The robustness of nonlinear schemes against photon and atom losses, inefficient detectors, damping, and atomic decoherence has been addressed in most of the proposals [2,3,5,9,10,14–16].

The conclusion is that for classical probes, practical imperfections lead to a reduction of sensitivity without affecting scaling with the number of particles [10]. In this context, there are

some differences between the conclusions of the analyses in Refs. 9 and 10, perhaps due to the different optimum probe considered.

5 Conclusions

We hope to have included all proposals introduced so far in the new area of quantum nonlinear metrology. These works confirm that nonlinear schemes allow us to put quantum limits farther than linear schemes. Much remains to be done, especially concerning experimental confirmations and applications, and extending its usefulness to a wider range of signals. To this end, a key point is the possibility of using classical probes because of their robustness against practical imperfections. In any case, we think that this issue provides a deeper understanding of quantum metrology.

6 Appendix A: Atom-Photon Equivalence

Bose-Einstein condensates and photons can be described alike in terms of annihilation operators or complex amplitude operators a_k with commutation relation $[a_k, a_\ell^\dagger] = \delta_{k,\ell}$. The index k typically represents internal energies, minima of trapping potentials, spin or polarization states, frequency, or spatial distributions, such as input, internal, or output arms of interferometers.

For two-mode situations, the following operators are especially useful [91,92]

$$\begin{aligned} \hat{N} = a_1^\dagger a_1 + a_2^\dagger a_2,\, J_x = \tfrac{1}{2}\big(a_2^\dagger a_1 + a_1^\dagger a_2\big), \\ J_y = \tfrac{i}{2}\big(a_2^\dagger a_1 - a_1^\dagger a_2\big),\, J_z = \tfrac{1}{2}\big(a_1^\dagger a_1 - a_2^\dagger a_2\big), \end{aligned} \tag{23}$$

satisfying the angular-momentum commutation relations

$$[J_k, J_\ell] = i \sum_{n=x,y,z} \epsilon_{k,\ell,n} J_n, \qquad [\hat{N}, \boldsymbol{J}] = \mathbf{0}, \tag{24}$$

with

$$J^2 = \frac{\hat{N}}{2}\left(\frac{\hat{N}}{2} + 1\right), \tag{25}$$

where $\epsilon_{k,\ell,n}$ is the fully antisymmetric tensor with $\epsilon_{x,y,z} = 1$. The operator $\hat{N}$ is the total number of particles, while J_z is proportional to the difference of the number of particles in the two modes. There is the following useful correspondence

$$|j, m\rangle = |n_1 = j + m\rangle |n_2 = j - m\rangle, \tag{26}$$

between the standard angular-momentum basis $|j, m\rangle$ of simultaneous eigenvectors of J_z and J^2, *i. e.*, $J_z|\, j, m\rangle = m|\, j, m\rangle,\ J^2|\, j, m\rangle = j(j+1)|\, j, m\rangle$, and the product of number states in the two modes $|n_1\rangle_1 |n_2\rangle_2$ with $a_j^\dagger a_j |n_j\rangle_j = n_j |n_j\rangle_j$.

For N two-level atoms, we can consider also the collective spin picture

$$\hat{N} = \sum_{k=1}^{N} \sigma_0^{(k)}, \quad \boldsymbol{J} = \frac{1}{2}\sum_{k=1}^{N} \boldsymbol{\sigma}^{(k)}, \tag{27}$$

where $\sigma^{(k)}$ are the Pauli matrices acting on the two-level space of the k'th particle spanned by $|\uparrow, \downarrow\rangle_k$

$$\begin{aligned} \sigma_0^{(k)} = |\uparrow\rangle_k\langle\uparrow| + |\downarrow\rangle_k\langle\downarrow|, \sigma_x^{(k)} = \tfrac{1}{2}\left(|\downarrow\rangle_k\langle\uparrow| + |\uparrow\rangle_k\langle\downarrow|\right), \\ \sigma_y^{(k)} = \tfrac{i}{2}\left(|\downarrow\rangle_k\langle\uparrow| - |\uparrow\rangle_k\langle\downarrow|\right), \sigma_z^{(k)} = \tfrac{1}{2}\left(|\uparrow\rangle_k\langle\uparrow| - |\downarrow\rangle_k\langle\downarrow|\right). \end{aligned} \tag{28}$$

7 Appendix B: Classical and Nonclassical States

Nonclassicality is a relevant issue in quantum metrology. The common wisdom is that the ultimate quantum limits can be approached exclusively by nonclassical or entangled states, this being a paradigm of practical applications of quantum physics.

7.1 *Classical States*

The most famous classical states, and the only ones that are pure states, are quadrature coherent states $|\alpha\rangle$, which are eigenstates of the complex amplitude operator $a|\alpha\rangle = \alpha|\alpha\rangle$ [93–96]. In the number basis read

$$|\alpha\rangle = e^{-|\alpha|^2/2} \sum_{n=0}^{\infty} \frac{\alpha^n}{\sqrt{n!}} |n\rangle. \tag{29}$$

The most general classical state is given by a random distribution of coherent states $|\alpha\rangle$, where the random amplitude α follows any real, positive, and normalized distribution $P(\alpha)$. Nevertheless, the classical/nonclassical frontier is somewhat misty [97–103].

Two-mode coherent states $|\alpha_1\rangle|\alpha_2\rangle$ define the SU(2) coherent states $|N, \Omega\rangle$ as [104,105]

$$|\alpha_1\rangle|\alpha_2\rangle = e^{-r^2/2} \sum_{N=0}^{\infty} \frac{r^N e^{iN\delta}}{\sqrt{N!}} |\, j = N/2, \Omega\rangle, \tag{30}$$

with (up to a global phase)

$$|\, j, \Omega\rangle = \sum_{m=-j}^{j} \begin{pmatrix} 2j \\ j+m \end{pmatrix}^{1/2} \left(\sin\frac{\theta}{2}\right)^{j+m} \left(\cos\frac{\theta}{2}\right)^{j-m} e^{-im\phi} |j, m\rangle, \tag{31}$$

where Ω represents the pair of state parameters θ, ϕ. The quadrature and SU(2) state parameters are connected by the relations

$$\alpha_1 = r \sin\frac{\theta}{2} e^{i\delta} e^{-i\phi}, \qquad \alpha_2 = r \cos\frac{\theta}{2} e^{i\delta}. \tag{32}$$

SU(2) coherent states are considered classical concerning just angular-momentum variables [106], but they are nonclassical from a wider two-mode perspective. For example, the polar SU(2) coherent states $\theta = 0,\ \pi$, are the product of number states $|n\rangle_1|0\rangle_2$, $|0\rangle_1|n\rangle_2$, and therefore nonclassical.

For distinguishable particles, the SU(2) coherent states factorize as the product of identical single-particle states

$$|\, j = N/2, \Omega\rangle = \bigotimes_{k=1}^{N} |j = 1/2, \Omega\rangle_k, \tag{33}$$

where $|\, j = N/2, \Omega\rangle_k$ are SU(2) coherent states for $j = 1/2$

$$|\, j = 1/2, \Omega\rangle = \sin\frac{\theta}{2} e^{-i\phi/2} |\uparrow\rangle_k + \cos\frac{\theta}{2} e^{i\phi/2} |\downarrow\rangle_k, \tag{34}$$

and it can be appreciated that for $j = 1/2$, every pure state is an SU(2) coherent state. This relation supports the general understanding of coherent states as unentangled, and accordingly, nonclassical states as entangled. In this regard, note that SU(2) coherent states are in general

mode-entangled in the sense that $|\, j, \Omega\rangle \neq |\psi_1\rangle_1 |\psi_2\rangle_2$, where $|\psi_j\rangle_j$ are arbitrary states in the corresponding mode a_j.

7.2 *Nonclassical States*

Most famous nonclassical states related to precision metrology are as follows.

1. Two-mode number states $|n_1\rangle_1 |n_2\rangle_2$, with $n_1 n_2 \neq 0$, this is to say $|\, j, m \neq \pm j\rangle$, especially cases with the same number of photons in each mode $|n\rangle_1 |n\rangle_2 = |\, j = n, m = 0\rangle$ [107–109], which can be regarded as the limit of SU(2) squeezed states [36,37,51–58].
2. Quadrature squeezed states: these are states with fluctuations of a rotated quadrature $X_\varphi = e^{i\varphi} a + e^{-i\varphi} a^\dagger$ smaller than for quadrature coherent states [93–95].
3. SU(2) squeezed states: there are several definitions of SU(2) or spin squeezing [36,37, 51–58]. The most meaningful criteria are based on the angular-momentum components $J_\perp$ orthogonal to the average vector $\langle \mathbf{J} \rangle$, so that by definition $\langle J_\perp \rangle = 0$. The general idea is that $\Delta J_\perp$, or a suitable function of $\Delta J_\perp$ and $|\langle \mathbf{J} \rangle|$, should be smaller than its value for SU(2) coherent states with $\langle J_\perp \rangle = 0$. From the single-particle perspective discussed before, SU(2) squeezing would imply entanglement.
4. Schrödinger cat states or N00N states [44–50]: these are coherent superpositions of distinguishable states of the form (in the number and spin bases)

$$\frac{1}{\sqrt{2}} \left(|n\rangle_1 |0\rangle_2 + |0\rangle_1 |n\rangle_2 \right) = \frac{1}{\sqrt{2}} \left(|j, j\rangle + |j, -j\rangle \right). \tag{35}$$

5. Phase states [92]: deep down, interferometry is related with phase-difference statistics. The states that represent this variable in the quantum domain are the phase-difference states

$$|j, \phi\rangle = \frac{1}{\sqrt{2j+1}} \sum_{m=-j}^{j} e^{-im\phi} |j, m\rangle. \tag{36}$$

   There are no simple procedures of generating or measuring these states, so that sometimes they are replaced by equatorial SU(2) coherent states $|\, j, \Omega\rangle$ with $\theta = \pi/2$ [110–112].

8 Appendix C: Data Analysis

In our context, our main interest is placed in the estimation of the signal uncertainty $\Delta\tilde{\chi}$, since this allows us to compare schemes with different generators and determine optimum probes and measurements. Throughout we assume that the signal χ is small enough to simplify some expressions by series expansions on powers of χ retaining just the lower one. This is justified, since quantum limits are usually concerned with the detection of very weak signals.

8.1 *Signal-to-Noise Ratio*

A convenient performance measure is the signal-to-noise ratio (see Fig. 3)

$$\frac{S}{N} = \sqrt{\nu} \frac{\left| \langle M \rangle_\chi - \langle M \rangle_0 \right|}{\Delta M} \simeq \chi \sqrt{\nu} \frac{\left| \frac{\partial \langle M \rangle_\chi}{\partial \chi} \right|_{\chi=0}}{\Delta M}, \tag{37}$$

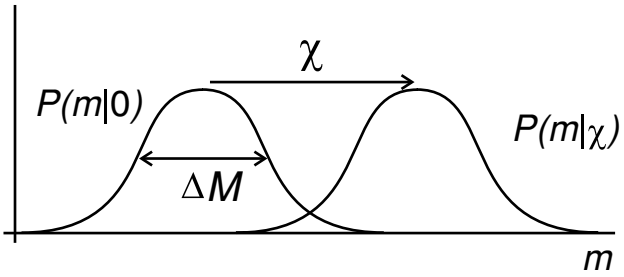

Fig. 3 Signal-induced shift χ of the statistics of the observable M.

where ΔM is the variance of M in the probe state $|\psi\rangle$, ν is the number of repetitions of the measurement (assumed independent), and we considered the weak-signal approximation

$$\langle M\rangle_\chi = \langle\psi_\chi|M|\psi_\chi\rangle \simeq \langle M\rangle_0 + \chi \left.\frac{\partial\langle M\rangle_\chi}{\partial\chi}\right|_{\chi=0}, \tag{38}$$

being

$$\left.\frac{\partial\langle M\rangle_\chi}{\partial\chi}\right|_{\chi=0} = |\langle\psi|[M,G]|\psi\rangle|. \tag{39}$$

The minimum signal that can be detected (referred to as $\Delta\tilde{\chi}$) can be estimated as the signal leading to unit signal-to-noise ratio

$$\frac{S}{N} = 1 \to \Delta\tilde{\chi} = \frac{\Delta M}{\sqrt{\nu}\left|\frac{\partial\langle M\rangle_\chi}{\partial\chi}\right|_{\chi=0}} \geq \frac{1}{2\sqrt{\nu}\Delta G}, \tag{40}$$

where the Heisenberg uncertainty relation has been used,

$$\Delta G\Delta M \geq \frac{1}{2}|\langle[M,G]\rangle| = \frac{1}{2}\left|\frac{\partial\langle M\rangle_\chi}{\partial\chi}\right|. \tag{41}$$

Equation (40) is essentially an error propagation in the inversion of Eq. (38),

$$\tilde{\chi} = \frac{\langle M\rangle_\chi - \langle M\rangle_0}{\left.\frac{\partial\langle M\rangle_\chi}{\partial\chi}\right|_{\chi=0}}. \tag{42}$$

In principle, from Eqs. (40) and (41) it seems that optimum resolution requires both equality in the uncertainty relation in Eq. (41) and maximum ΔG. However, these two conditions may be not compatible [16].

The main advantage of the signal-to-noise ratio is simplicity, allowing meaningful conclusions with very simple calculus. Nevertheless, relevant situations are excluded. For example, it may happen that $\langle M\rangle_\chi = 0$ for all χ. This holds in linear schemes for relevant probes such as $|j,0\rangle$ and $|j,j\rangle + |j,-j\rangle$. This might be avoided by considering that $\langle M^k\rangle_\chi \neq 0$ for a suitable integer k (otherwise, the measurement would be useless). Moreover, $\langle M\rangle_\chi$ may be a periodic function of χ, so that no single $\tilde{\chi}$ can be inferred from Eqs. (38) or (42), for example (see Sec. 4.3).

8.2 *Fisher Information*

A more powerful analysis considers a Bayesian strategy to get a probability distribution representing our knowledge about the signal after the outcome m in the measurement of M as [65,113–120]

$$P(\chi|m) \propto P(m|\chi)P(\chi), \tag{43}$$

where $P(\chi)$ is the prior information about χ that may include the outcomes of previous measurements. The posterior distribution $P(\chi|m)$ can be used to infer the best value for χ and its uncertainty, for example via a maximum likelihood strategy.

In any case, the minimum uncertainty of any unbiased and efficient estimator $\tilde{\chi}$ is given by the Cramer-Rao lower bound [65,113–118]

$$\Delta\tilde{\chi} = \frac{1}{\sqrt{\nu F}}, \qquad F = \sum_m \frac{1}{P(m|\chi)} \left(\frac{\partial P(m|\chi)}{\partial \chi} \right)^2, \tag{44}$$

where F is the Fisher information. This is a measure of the information that m provides about χ. In particular, the Cramer-Rao lower bound coincides with the signal-to-noise ratio in Eq. (40) when $P(m|\chi)$ is a Gaussian with a width independent of χ (assuming for simplicity that m is a continuous variable)

$$P(m|\chi) = \frac{1}{\sqrt{2\pi}\,\Delta M} \exp\left[-\frac{\left(m - \langle M \rangle_\chi\right)^2}{2\left(\Delta M\right)^2} \right], \tag{45}$$

while in general [35]

$$\frac{\Delta M}{\left| \frac{\partial \langle M \rangle_\chi}{\partial \chi} \right|} \geq \frac{1}{\sqrt{F}}, \tag{46}$$

where equality is reached for the minimum uncertainty states of Eq. (41) [see Eq. (52)].

The signal-to-noise ratio in Eq. (37) is a measure of how close $\langle M \rangle_\chi$ and $\langle M \rangle_0$ are. Equivalently, the Fisher information is a measure of how close $P(m|\chi)$ and $P(m|\chi = 0)$ are. For small enough χ

$$\frac{1}{2} \sum_m \left[\sqrt{P(m|\chi)} - \sqrt{P(m|0)} \right]^2 = 1 - \sum_m \sqrt{P(m|\chi)P(m|0)} \simeq \frac{1}{8}\chi^2 F. \tag{47}$$

8.3 *Quantum Fisher Information and Intrinsic Resolution*

The two previous performance measures naturally depend on the actual measurement M performed. It can be also interesting to use assessments independent of M, representing the optimum results that can be obtained with any measurement. This can be addressed by considering the distance between the input $|\psi\rangle$ and output $|\psi_\chi\rangle$ probe states. For example, in terms of the corresponding density matrices ρ and ρ_χ, the Bures distance gives [119,120]

$$D^2 = 1 - \mathrm{tr}\left(\sqrt{\rho}\rho_\chi \sqrt{\rho} \right)^{1/2} \simeq \frac{1}{8}\chi^2 F_Q, \qquad F_Q = 2 \sum_{k,\ell} \frac{(p_k - p_\ell)^2}{p_k + p_\ell} \left| \langle \psi_k | G | \psi_\ell \rangle \right|^2, \tag{48}$$

where p_k, $|\psi_k\rangle$ are the eigenvalues and eigenvectors, respectively, of ρ (for a simpler alternative via the Hilbert-Schmidt distance, see Ref. 85). It is worth noting that in general, F_Q does not depend on χ [121].

F_Q is the maximum F over all possible measurements M, so that $F \leq F_Q$ [119], and the following quantum Cramer-Rao minimum uncertainty holds [79,117–119]

$$\Delta\tilde{\chi} = \frac{1}{\sqrt{\nu F_Q}}. \tag{49}$$

Since

$$F_Q \leq 4\,(\Delta G)^2\,, \tag{50}$$

where the equality holds for pure states, the minimum uncertainty scales as [119,120]

$$\Delta\tilde{\chi} = \frac{1}{2\sqrt{\nu}\Delta G}, \tag{51}$$

so that the quantum Cramer-Rao lower bound seemingly leads to the same conclusion of the signal-to-noise ratio in Eq. (40), but without involving the uncertainty relation in Eq. (41).

Finally, the previous performance measures satisfy the following chain of inequalities [35]

$$\frac{\Delta M}{\left|\frac{\partial\langle M\rangle_\chi}{\partial\chi}\right|} \geq \frac{1}{\sqrt{F}} \geq \frac{1}{\sqrt{F_Q}} \geq \frac{1}{2\Delta G}, \tag{52}$$

where all equalities are satisfied simultaneously for the minimum uncertainty states of Eq. (41).

Acknowledgments

We thank T. Alieva for encouraging this work and A. Rivas for valuable comments. This work has been supported by project number FIS2008-01267 of the Spanish Dirección General de Investigación del Ministerio de Ciencia e Innovación, and QUITEMAD S2009-ESP-1594 of the Consejería de Educación de la Comunidad de Madrid.

References

[1] A. Luis, "Phase-shift amplification for precision measurements without nonclassical states," *Phys. Rev. A* **65**, 025802 (2002).
[2] A. Luis, "Reaching quantum limits for phase-shift detection with semiclassical states," *J. Opt. B: Quantum Semiclassical Opt.* **6**, 1–4 (2004).
[3] A. Luis, "Heisenberg limit for displacements with semiclassical states," *Phys. Rev. A* **69**, 044101 (2004).
[4] A. Luis, "Nonlinear transformations and the Heisenberg limit," *Phys. Lett. A* **329**, 8–13 (2004).
[5] J. Beltrán and A. Luis, "Breaking the Heisenberg limit with inefficient detectors," *Phys. Rev. A* **72**, 045801 (2005).
[6] S. Boixo, S. T. Flammia, C. M. Caves, and J. M. Geremia, "Generalized limits for single-parameter quantum estimation," *Phys. Rev. Lett.* **98**, 090401 (2007).
[7] A. Luis, "Quantum limits, nonseparable transformations, and nonlinear optics," *Phys. Rev. A* **76**, 035801 (2007).
[8] C. C. Gerry, A. Benmoussa, and R. A. Campos, "Parity measurements, Heisenberg limited phase estimation, and beyond," *J. Mod. Opt.* **54**, 2177–2184 (2007).
[9] A. M. Rey, L. Jiang, and M. D. Lukin, "Quantum-limited measurements of atomic scattering properties," *Phys. Rev. A* **76**, 053617 (2007).
[10] S. Boixo, A. Datta, S. T. Flammia, A. Shaji, E. Bagan, and C. M. Caves, "Quantum-limited metrology with product states," *Phys. Rev. A* **77**, 012317 (2008).

[11] S. Choi and B. Sundaram, "Bose-Einstein condensate as a nonlinear Ramsey interferometer operating beyond the Heisenberg limit," *Phys. Rev. A* **77**, 053613 (2008).
[12] S. M. Roy and S. L. Braunstein, "Exponentially enhanced quantum metrology," *Phys. Rev. Lett.* **100**, 220501 (2008).
[13] S. Boixo, A. Datta, M. J. Davis, S. T. Flammia, A. Shaji, and C. M. Caves, "Quantum metrology: dynamics versus entanglement," *Phys. Rev. Lett.* **101**, 040403 (2008).
[14] M. J. Woolley, G. J. Milburn, and C. M. Caves, "Nonlinear quantum metrology using coupled nanomechanical resonators," *New J. Phys.* **10**, 125018 (2008).
[15] S. Boixo, A. Datta, M. J. Davis, A. Shaji, A. B. Tacla, and C. M. Caves, "Quantum-limited metrology and Bose-Einstein condensates," *Phys. Rev. A* **80**, 032103 (2009).
[16] D. Maldonado-Mundo and A. Luis, "Metrological resolution and minimum uncertainty states in linear and nonlinear signal detection schemes," *Phys. Rev. A* **80**, 063811 (2009).
[17] B. A. Chase, H. L. Partner, B. D. Black, B. Q. Baragiola, R. L. Cook, and J. M. Geremia, "Magnetic field estimation at and beyond 1/N scaling via an effective nonlinearity," e-print arXiv:quant-ph/0708.2730.
[18] B. A. Chase, B. Q. Baragiola, H. L. Partner, B. D. Black, and J. M. Geremia, "Magnetometry via a double-pass continuous quantum measurement of atomic spin," *Phys. Rev. A* **79**, 062107 (2009).
[19] S. Boixo, A. Datta, M. J. Davis, S. T. Flammia, A. Shaji, A. B. Tacla, and C. M. Caves, "Quantum metrology with Bose-Einstein condensates," *9th Intl. Conf. Quantum Commun. Measure. Comput. (QCMC) AIP Conf. Proc.* **1110**, 423–426 (2009).
[20] S. Boixo, A. Datta, M. J. Davis, S. T. Flammia, A. Shaji, A. B. Tacla, and C. M. Caves, "Quantum metrology from an information theory perspective," *9th Intl. Conf. Quantum Commun. Measure. Comput. (QCMC) AIP Conf. Proc.* **1110**, 427–432 (2009).
[21] A. Rivas and A. Luis, "Metrological resolution and nonclassicality in linear and nonlinear detection schemes," *Phys. Rev. Lett.* **105**, 010403 (2010).
[22] M. Napolitano and M. W. Mitchell, "Scaling and sensitivity in linear and nonlinear metrology of atomic spins," e-print arXiv:quant-ph/0910.5869v2.
[23] T. Tilma, S. Hamaji, W. J. Munro, and K. Nemoto, "Entanglement is not a critical resource for quantum metrology," *Phys. Rev. A* **81**, 022108 (2010).
[24] M. Zwierz, C. A. Perez-Delgado, and P. Kok, "General optimality of the Heisenberg limit for quantum metrology," e-print arXiv:quant-ph/1004.3944.
[25] M. Napolitano, N. Behbood, B. Dubost, M. Koschorrek, R. Sewell, and M.W. Mitchell, "Nonlinear metrology of atomic spins," 17th Central European Workshop on Quantum Optics, St. Andrews, Scotland, UK, 6-11 June 2010.
[26] P. A. M. Dirac, *The Principles of Quantum Mechanics*, Clarendon, Oxford, UK (1954).
[27] A. S. Lane, S. L. Braunstein, and C. M. Caves, "Maximum-likelihood statistics of multiple quantum phase measurements," *Phys. Rev. A* **47**, 1667–1696 (1992).
[28] V. Giovannetti, S. Lloyd, and L. Maccone, "Quantum metrology," *Phys. Rev. Lett.* **96**, 010401 (2006).
[29] V. Giovannetti, S. Lloyd, and L. Maccone, "Quantum-enhanced measurements: beating the standard quantum limit," *Science* **306**, 1330–1336 (2004).
[30] C. M. Caves, "Quantum-mechanical noise in an interferometer," *Phys. Rev. D* **23**, 1693–1708 (1981).
[31] B. Yurke, S. L. McCall, and J. R. Klauder, "SU(2) and SU(1,1) interferometers," *Phys. Rev. A* **33**, 4033–4054 (1986).
[32] B. C. Sanders and G. J. Milburn, "Optimal quantum measurements for phase estimation," *Phys. Rev. Lett.* **75**, 2944–2947 (1995).
[33] J. P. Dowling, "Correlated input-port, matter-wave interferometer: quantum-noise limits to the atom-laser gyroscope," *Phys. Rev. A* **57**, 4736–4746 (1998).
[34] H. Lee, P. Kok, and J. P. Dowling, "A quantum Rosetta stone for interferometry," *J. Mod. Opt.* **49**, 2325–2338 (2002).

[35] H. Uys and P. Meystre, "Quantum states for Heisenberg-limited interferometry," *Phys. Rev. A* **76**, 013804 (2007).
[36] D. J. Wineland, J. J. Bollinger, W. M. Itano, F. L. Moore, and D. J. Heinzen, "Spin squeezing and reduced quantum noise in spectroscopy," *Phys. Rev. A* **46**, R6797-R6800 (1992).
[37] D. J. Wineland, J. J. Bollinger, W. M. Itano, and D. J. Heinzen, "Squeezed atomic states and projection noise in spectroscopy," *Phys. Rev. A* **50**, 67–88 (1994).
[38] Z. Y. Ou, "Complementarity and fundamental limit in precision phase measurement," *Phys. Rev. Lett.* **77**, 2352–2355 (1996).
[39] Z. Y. Ou, "Fundamental quantum limit in precision phase measurement," *Phys. Rev. A* **55**, 2598–2609 (1997).
[40] D. W. Berry, B. L. Higgins, S. D. Bartlett, M. W. Mitchell, G. J. Pryde, and H. M. Wiseman, "How to perform the most accurate possible phase measurements," *Phys. Rev. A* **80**, 052114 (2009).
[41] L. Pezzé and A. Smerzi, "Sub shot-noise interferometric phase sensitivity with beryllium ions Schrödinger cat states," *Europhys. Lett.* **78**, 30004 (2007).
[42] B. L. Higgins, D. W. Berry, S. D. Bartlett, H. M. Wiseman, and G. J. Pryde, "Entanglement-free Heisenberg-limited phase estimation," *Nature* **450**, 393–396 (2007).
[43] B. L. Higgins, D. W. Berry, S. D. Bartlett, M. W. Mitchell, H. M. Wiseman, and G. J. Pryde, "Demonstrating Heisenberg-limited unambiguous phase estimation without adaptive measurements," *New J. Phys.* **11**, 073023 (2009).
[44] N. D. Mermin, "Extreme quantum entanglement in a superposition of macroscopically distinct states," *Phys. Rev. Lett.* **65**, 1838–1840 (1990).
[45] J. J Bollinger, W. M. Itano, D. J. Wineland, and D. J. Heinzen, "Optimal frequency measurements with maximally correlated states," *Phys. Rev. A* **54**, R4649-R4652 (1996).
[46] M. Brune, E. Hagley, J. Dreyer, X. Maître, A. Maali, C. Wunderlich, J. M. Raimond, and S. Haroche, "Observing the progressive decoherence of the "meter" in a quantum measurement," *Phys. Rev. Lett.* **77**, 4887–4890 (1996).
[47] C. C. Gerry and P. L. Knight, "Quantum superpositions and Schrödinger cat states in quantum optics," *Am. J. Phys.* **65**, 964–974 (1997).
[48] M. W. Mitchel, J. S. Lundeen, and A. M. Steinberg, "Super-resolving phase measurements with a multiphoton entangled state," *Nature (London)* **429**, 161–164 (2004).
[49] D. Leibfried, E. Knill, S. Seidelin, J. Britton, R. B. Blakestad, J. Chiaverini, D. B. Hume, W. M. Itano, J. D. Jost, C. Langer, R. Ozeri, R. Reichle, and D. J. Wineland, "Creation of a six-atom Schrödinger cat state," *Nature (London)* **438**, 639–642 (2005).
[50] T. Nagata, R. Okamoto, J. L. O'Brien, K. Sasaki, and S. Takeuchi, "Beating the standard quantum limit with four-entangled photons," *Science* **316**, 726–729 (2007).
[51] M. Kitagawa and M. Ueda, "Squeezed spin states," *Phys. Rev. A* **47**, 5138–5143 (1993).
[52] M. Hillery and L. Mlodinow, "Interferometers and minimum-uncertainty states," *Phys. Rev. A* **48**, 1548–1558 (1993).
[53] G. S. Agarwal and R. R. Puri, "Atomic states with spectroscopic squeezing," *Phys. Rev. A* **49**, 4968–4971 (1994).
[54] C. Brif and A. Mann, "Nonclassical interferometry with intelligent light," *Phys. Rev. A* **54**, 4505–4518 (1996).
[55] J. Hald, J. L. Sørensen, C. Schori, and E. S. Polzik, "Spin squeezed atoms: a macroscopic entangled ensemble created by light," *Phys. Rev. Lett.* **83**, 1319–1322 (1999).
[56] A. S. Sørensen and K. Mølmer, "Entanglement and extreme spin squeezing," *Phys. Rev. Lett.* **86**, 4431–4434 (2001).
[57] A. Luis and N. Korolkova, "Polarization squeezing and nonclassical properties of light," *Phys. Rev. A* **74**, 043817 (2006).
[58] J. Estéve, C. Gross, A. Weller, S. Giovanazzi, and M. K. Oberthaler, "Squeezing and entanglement in a Bose–Einstein condensate," *Nature (London)* **455**, 1216–1219 (2008).

[59] J. K. Korbicz, J. I. Cirac, and M. Lewenstein "Spin squeezing inequalities and entanglement of N qubit states," *Phys. Rev. Lett.* **95**, 120502 (2005).
[60] C. M. Caves, "Quantum-mechanical radiation-pressure fluctuations in an interferometer," *Phys. Rev. Lett.* **45**, 75–79 (1980).
[61] T. Rudolph and L. Grover, "Quantum communication complexity of establishing a shared reference frame," *Phys. Rev. Lett.* **91**, 217905 (2003).
[62] M. de Burgh and S. D. Bartlett, "Quantum methods for clock synchronization: beating the standard quantum limit without entanglement," *Phys. Rev. A* **72**, 042301 (2005).
[63] P. M. Anisimov, G. M. Raterman, A. Chiruvelli, W. N. Plick, S. D. Huver, H. Lee, and J. P. Dowling, "Quantum metrology with two-mode squeezed vacuum: parity detection beats the Heisenberg limit," *Phys. Rev. Lett.* **104**, 103602 (2010).
[64] Z. Hradil and J. H. Shapiro, "Quantum phase measurements with infinite peak-likelihood and zero phase information," *Quantum Opt.* **4**, 31–37 (1992).
[65] S. L. Braunstein, A. S. Lane, and C. M. Caves, "Maximum-likelihood analysis of multiple quantum phase measurements," *Phys. Rev. Lett.* **69**, 2153–2156 (1992).
[66] I Bialynicki-Birula and J. Mycielski, "Uncertainty relations for information entropy in wave mechanics," *Commun. Math. Phys.* **44**, 129–132 (1975).
[67] D. Deutsch, "Uncertainty in quantum measurements," *Phys. Rev. Lett.* **50**, 631–633 (1983).
[68] K. Kraus, "Complementary observables and uncertainty relations," *Phys. Rev. D* **35**, 3070–3075 (1987).
[69] H. Maassen and J. B. M. Uffink, "Generalized entropic uncertainty relations," *Phys. Rev. Lett.* **60**, 1103–1106 (1988).
[70] U. Larsen, "Superspace geometry: the exact uncertainty relationship between complementary aspects," *J. Phys. A* **23**, 1041–1061 (1990).
[71] G. N. Lawrence, "Proposed international standard for laser beam quality falls short," *Laser Focus World* **30**, 109–114 (1994).
[72] M. J. W. Hall, "Universal geometric approach to uncertainty, entropy, and information," *Phys. Rev. A* **59**, 2602–2615 (1999).
[73] J. Hilgevoord, "The standard deviation is not an adequate measure of quantum uncertainty," *Am. J. Phys.* **70**, 983–983 (2002).
[74] J. Řeháček and Z. Hradil, "Uncertainty relations from Fisher information," *J. Mod. Opt.* **51**, 979–982 (2004).
[75] I. Bialynicki-Birula, "Formulation of the uncertainty relations in terms of the Rényi entropies," *Phys. Rev. A* **74**, 052101 (2006).
[76] A. Luis, "Gaussian beams and minimum diffraction," *Opt. Lett.* **31**, 3644–3646 (2006).
[77] A. Luis, "Quantum properties of exponential states," *Phys. Rev. A* **75**, 052115 (2007).
[78] S. Zozor, M. Portesi, and C. Vignat, "Some extensions of the uncertainty principle," *Physica A* **387**, 4800–4808 (2008).
[79] S. L. Braunstein, C. M. Caves, and G. J. Milburn, "Generalized uncertainty relations: theory, examples, and Lorentz invariance," *Ann. Phys.* (NY) **247**, 135–173 (1996).
[80] A. Kuzmich, N. P. Bigelow, and L. Mandel, "Atomic quantum non-demolition measurements and squeezing," *Europhys. Lett.* **42**, 481–486 (1998).
[81] A. Kuzmich, L. Mandel, and N. P. Bigelow, "Generation of spin squeezing via continuous quantum nondemolition measurement," *Phys. Rev. Lett.* **85**, 1594–1597 (2000).
[82] T. Takano, S.-I.-R Tanaka, R. Namiki, and Y. Takahashi, "Manipulation of nonclassical atomic spin states," *Phys. Rev. Lett.* **104**, 013602 (2010).
[83] L. Pezzé and A. Smerzi, "Entanglement, nonlinear dynamics, and the Heisenberg limit," *Phys. Rev. Lett.* **102**, 100401 (2009).
[84] P. Hyllus, L. Pezzé, and A. Smerzi, "Entanglement and sensitivity in precision measurements with states of a fluctuating number of particles," e-print arXiv:quant-ph/1003.0649.
[85] A. Rivas and A. Luis, "Intrinsic metrological resolution as a distance measure and nonclassical light," *Phys. Rev. A* **77**, 063813 (2008).

[86] A. Rivas and A. Luis, private communication (2010).
[87] S. F. Huelga, C. Macchiavello, T. Pellizzari, A. K. Ekert, M. B. Plenio, and J. I. Cirac, "Improvement of frequency standards with quantum entanglement," *Phys. Rev. Lett.* **79**, 3865–3868 (1997).
[88] M. A. Rubin and S. Kaushik, "Loss-induced limits to phase measurement precision with maximally entangled states," *Phys. Rev. A* **75**, 053805 (2007).
[89] G. Gilbert, M. Hamrick, and Y. S. Weinstein, "Use of maximally entangled N-photon states for practical quantum interferometry," *J. Opt. Soc. Am. B* **25**, 1336–1340 (2008).
[90] U. Dorner, R. Demkowicz-Dobrzanski, B. J. Smith, J. S. Lundeen, W. Wasilewski, K. Banaszek, and I. A. Walmsley, "Optimal quantum phase estimation," *Phys. Rev. Lett.* **102**, 040403 (2009).
[91] J. Schwinger, *Quantum Theory of Angular Momentum*, Academic Press, New York (1965).
[92] A. Luis and L. L. Sánchez-Soto, "Quantum phase difference, phase measurements and Stokes operators," in *Prog. Opt.* **41**, 421–481 (2000).
[93] L. Mandel and E. Wolf, *Optical Coherence and Quantum Optics*, Cambridge University Press, Cambridge, England (1995).
[94] M. O. Scully and M. S. Zubairy, *Quantum Optics*, Cambridge University Press, Cambridge, England (1997).
[95] C. C. Gerry and P. L. Knight, *Introductory Quantum Optics*, Cambridge University Press, Cambridge, England (2005).
[96] J. R. Klauder and B.S. Skagerstam, *Coherent States: Applications in Physics and Mathematical Physics*, World Scientific, Singapore (1985).
[97] J. A. Vaccaro, "New Wigner function for number and phase," *Opt. Commun.* **113**, 421–426 (1995).
[98] J. A. Vaccaro, "Number-phase Wigner function on Fock space," *Phys. Rev. A* **52**, 3474–3488 (1995).
[99] J. A. Vaccaro and D. T. Pegg, "Wigner function for number and phase," *Phys. Rev. A* **41**, 5156–5163 (1990).
[100] L. M. Johansen, "Nonclassical properties of coherent states," *Phys. Lett. A* **329**, 184–187 (2004).
[101] L. M. Johansen, "Nonclassicality of thermal radiation," *J. Opt. B: Quantum Semiclassical Opt.* **6**, L21-L24 (2004).
[102] L. M. Johansen and A. Luis, "Nonclassicality in weak measurements," *Phys. Rev. A* **70**, 052115 (2004).
[103] A. Luis, "Nonclassical polarization states," *Phys. Rev. A* **73**, 063806 (2006).
[104] F. T. Arecchi, E. Courtens, R. Gilmore, and H. Thomas, "Atomic coherent states in quantum optics," *Phys. Rev. A* **6**, 2211–2237 (1972).
[105] P. W. Atkins and J. C. Dobson, "Angular momentum coherent states," *Proc. R. Soc. London Ser. A* **321**, 321–340 (1971).
[106] O. Giraud, P. Braun, and D. Braun, "Classicality of spin states," *Phys. Rev. A* **78**, 042112 (2008).
[107] J. G. Rarity, P. R. Tapster, E. Jakeman, T. Larchuk, R. A. Campos, M. C. Teich, and B. E. A. Saleh, "Two-photon interference in a Mach-Zehnder interferometer," *Phys. Rev. Lett.* **65**, 1348–1351 (1990).
[108] M. J. Holland and K. Burnett, "Interferometric detection of optical phase shifts at the Heisenberg limit," *Phys. Rev. Lett.* **71**, 1355–1358 (1993).
[109] P. Bouyer and M. A. Kasevich, "Heisenberg-limited spectroscopy with degenerate Bose-Einstein gases," *Phys. Rev. A* **56**, R1083-R1086 (1997).
[110] A. J. Leggett and F. Sols, "On the concept of spontaneously broken gauge symmetry in condensed matter physics," *Found. Phys.* **21**, 353–364 (1991).
[111] Y. Castin and J. Dalibard, "Relative phase of two Bose-Einstein condensates," *Phys. Rev. A* **55**, 4330–4337 (1997).

[112] A. Sinatra and Y. Castin, "Phase dynamics of Bose-Einstein condensates: losses versus revivals," *Eur. Phys. J. D* **4**, 247–260 (1998).
[113] S. L. Braunstein, "Quantum limits on precision measurements of phase," *Phys. Rev. Lett.* **69**, 3598–3601 (1992).
[114] B. R. Frieden, "Fisher information and uncertainty complementarity," *Phys. Lett. A* **169**, 123–130 (1992).
[115] B. R. Frieden, *Physics from Fisher Information: A Unification*, Cambridge University Press, Cambridge, England (1998).
[116] Z. Hradil and J. Řeháček, "Quantum interference and Fisher information," *Phys. Lett. A* **334**, 267–272 (2005).
[117] C. W. Helstrom, *Quantum Detection and Estimation Theory*, Academic Press, New York (1976).
[118] A. S. Holevo, *Probabilistic and Statistical Aspects of Quantum Theory*, North-Holland, Amsterdam (1982).
[119] S. L. Braunstein and C. M. Caves, "Statistical distance and the geometry of quantum states," *Phys. Rev. Lett.* **72**, 3439–3443 (1994).
[120] S. Luo and Q. Zhang, "Informational distance on quantum-state space," *Phys. Rev. A* **69**, 032106 (2004).
[121] L. Pezzé and A. Smerzi, "Mach-Zehnder interferometry at the Heisenberg limit with coherent and squeezed-vacuum light," *Phys. Rev. Lett.* **100**, 073601 (2008).

Alfredo Luis received his MS degree in physics from the University of Zaragoza in 1986, and his PhD degree in physics from the University Complutense in 1992. His current research interests include quantum optical topics such as metrology, nonclassical states of light, uncertainty relations, complementarity, and also polarization and coherence for classical vectorial waves.